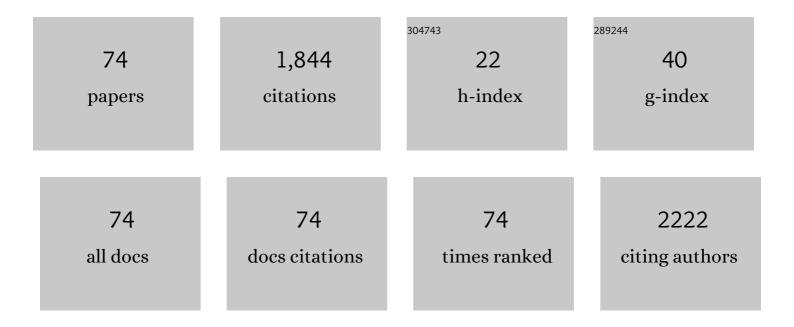
## **Thomas Wanek**

List of Publications by Year in descending order

Source: https://exaly.com/author-pdf/2588222/publications.pdf Version: 2024-02-01



#	Article	IF	CITATIONS
1	PET imaging to assess the impact of P-glycoprotein on pulmonary drug delivery in rats. Journal of Controlled Release, 2022, 342, 44-52.	9.9	11
2	Use of PET Imaging to Assess the Efficacy of Thiethylperazine to Stimulate Cerebral MRP1 Transport Activity in Wild-Type and APP/PS1-21 Mice. International Journal of Molecular Sciences, 2022, 23, 6514.	4.1	2
3	Impact of P-gp and BCRP on pulmonary drug disposition assessed by PET imaging in rats. Journal of Controlled Release, 2022, 349, 109-117.	9.9	5
4	Complete inhibition of ABCB1 and ABCG2 at the blood–brain barrier by co-infusion of erlotinib and tariquidar to improve brain delivery of the model ABCB1/ABCG2 substrate [ <sup>11</sup> C]erlotinib. Journal of Cerebral Blood Flow and Metabolism, 2021, 41, 1634-1646.	4.3	17
5	Lipophilicity and Click Reactivity Determine the Performance of Bioorthogonal Tetrazine Tools in Pretargeted <i>In Vivo</i> Chemistry. ACS Pharmacology and Translational Science, 2021, 4, 824-833.	4.9	45
6	Assessing the Functional Redundancy between P-gp and BCRP in Controlling the Brain Distribution and Biliary Excretion of Dual Substrates with PET Imaging in Mice. Pharmaceutics, 2021, 13, 1286.	4.5	7
7	Influence of ABC transporters on the excretion of ciprofloxacin assessed with PET imaging in mice. European Journal of Pharmaceutical Sciences, 2021, 163, 105854.	4.0	7
8	Characterization of an APP/tau rat model of Alzheimer's disease by positron emission tomography and immunofluorescent labeling. Alzheimer's Research and Therapy, 2021, 13, 175.	6.2	8
9	Age dependency of cerebral P-glycoprotein function in wild-type and APPPS1 mice measured with PET. Journal of Cerebral Blood Flow and Metabolism, 2020, 40, 150-162.	4.3	20
10	Measurement of cerebral ABCC1 transport activity in wild-type and APP/PS1-21 mice with positron emission tomography. Journal of Cerebral Blood Flow and Metabolism, 2020, 40, 954-965.	4.3	14
11	In vivo characterization of [18F]AVT-011 as a radiotracer for PET imaging of multidrug resistance. European Journal of Nuclear Medicine and Molecular Imaging, 2020, 47, 2026-2035.	6.4	3
12	Imaging P-Glycoprotein Induction at the Blood–Brain Barrier of a β-Amyloidosis Mouse Model with <sup>11</sup> C-Metoclopramide PET. Journal of Nuclear Medicine, 2020, 61, 1050-1057.	5.0	21
13	Measurement of Hepatic ABCB1 and ABCC2 Transport Activity with [11C]Tariquidar and PET in Humans and Mice. Molecular Pharmaceutics, 2020, 17, 316-326.	4.6	15
14	Brain Distribution of Dual ABCB1/ABCG2 Substrates Is Unaltered in a Beta-Amyloidosis Mouse Model. International Journal of Molecular Sciences, 2020, 21, 8245.	4.1	4
15	Impact of Attenuation Correction on Quantification Accuracy in Preclinical Whole-Body PET Images. Frontiers in Physics, 2020, 8, .	2.1	0
16	Plasma pharmacokinetic and metabolism of [18F]THK-5317 are dependent on sex. Nuclear Medicine and Biology, 2020, 84-85, 28-32.	0.6	5
17	Correlated Multimodal Imaging in Life Sciences: Expanding the Biomedical Horizon. Frontiers in Physics, 2020, 8, .	2.1	61
18	Assessing the Activity of Multidrug Resistance–Associated Protein 1 at the Lung Epithelial Barrier. Journal of Nuclear Medicine, 2020, 61, 1650-1657.	5.0	16

THOMAS WANEK

#	Article	IF	CITATIONS
19	Inhibition of ABCB1 and ABCG2 at the Mouse Blood–Brain Barrier with Marketed Drugs To Improve Brain Delivery of the Model ABCB1/ABCG2 Substrate [ <sup>11</sup> C]erlotinib. Molecular Pharmaceutics, 2019, 16, 1282-1293.	4.6	20
20	Generation and Characterization of an <i>Abcc1</i> Humanized Mouse Model ( <i>hABCC1<sup>flx/flx</sup></i> ) with Knockout Capability. Molecular Pharmacology, 2019, 96, 138-147.	2.3	4
21	Reproducibility and Comparability of Preclinical PET Imaging Data: A Multicenter Small-Animal PET Study. Journal of Nuclear Medicine, 2019, 60, 1483-1491.	5.0	20
22	Crossâ€Isotopic Bioorthogonal Tools as Molecular Twins for Radiotheranostic Applications. ChemBioChem, 2019, 20, 1530-1535.	2.6	6
23	PET imaging of the mouse brain reveals a dynamic regulation of SERT density in a chronic stress model. Translational Psychiatry, 2019, 9, 80.	4.8	7
24	Influence of Multidrug Resistance-Associated Proteins on the Excretion of the ABCC1 Imaging Probe 6-Bromo-7-[11C]Methylpurine in Mice. Molecular Imaging and Biology, 2019, 21, 306-316.	2.6	15
25	Influence of breast cancer resistance protein and P-glycoprotein on tissue distribution and excretion of Ko143 assessed with PET imaging in mice. European Journal of Pharmaceutical Sciences, 2018, 115, 212-222.	4.0	4
26	Comparison of fully-automated radiosyntheses of [11C]erlotinib for preclinical and clinical use starting from in target produced [11C]CO2 or [11C]CH4. EJNMMI Radiopharmacy and Chemistry, 2018, 3, 8.	3.9	10
27	EGFR is required for FOSâ€dependent bone tumor development via RSK2/CREB signaling. EMBO Molecular Medicine, 2018, 10, .	6.9	24
28	Humanization of the blood–brain barrier transporter ABCB1 in mice disrupts genomic locus — lessons from three unsuccessful approaches. European Journal of Microbiology and Immunology, 2018, 8, 78-86.	2.8	2
29	Effect of Rifampicin on the Distribution of [ <sup>11</sup> C]Erlotinib to the Liver, a Translational PET Study in Humans and in Mice. Molecular Pharmaceutics, 2018, 15, 4589-4598.	4.6	17
30	Hepatocyte-Specific Deletion of EGFR in Mice Reduces Hepatic Abcg2 Transport Activity Measured by [11C]erlotinib and Positron Emission Tomography. Drug Metabolism and Disposition, 2017, 45, 1093-1100.	3.3	11
31	[18F]Fluoroalkyl azides for rapid radiolabeling and (Re)investigation of their potential towards in vivo click chemistry. Organic and Biomolecular Chemistry, 2017, 15, 5976-5982.	2.8	13
32	On the applicability of [18F]FBPA to predict L-BPA concentration after amino acid preloading in HuH-7 liver tumor model and the implication for liver boron neutron capture therapy. Nuclear Medicine and Biology, 2017, 44, 83-89.	0.6	14
33	Strategies to Inhibit ABCB1- and ABCG2-Mediated Efflux Transport of Erlotinib at the Blood–Brain Barrier: A PET Study on Nonhuman Primates. Journal of Nuclear Medicine, 2017, 58, 117-122.	5.0	43
34	[ 11 C]Erlotinib PET cannot detect acquired erlotinib resistance in NSCLC tumor xenografts in mice. Nuclear Medicine and Biology, 2017, 52, 7-15.	0.6	6
35	32nd International Austrian Winter Symposium. EJNMMI Research, 2016, 6, 32.	2.5	0
36	Synthesis and preclinical characterization of 1-(6′-deoxy-6′-[ 18 F]fluoro-β- d) Tj ETQq0 0 0 rgBT /Overloc assess tumor hypoxia. Bioorganic and Medicinal Chemistry, 2016, 24, 5326-5339.	k 10 Tf 50 ( 3.0	67 Td (-allofu 13

THOMAS WANEK

#	Article	IF	CITATIONS
37	Preloading with L-BPA, L-tyrosine and L-DOPA enhances the uptake of [18F]FBPA in human and mouse tumour cell lines. Applied Radiation and Isotopes, 2016, 118, 67-72.	1.5	12
38	Design, Synthesis, and Evaluation of a Low-Molecular-Weight <sup>11</sup> C-Labeled Tetrazine for Pretargeted PET Imaging Applying Bioorthogonal in Vivo Click Chemistry. Bioconjugate Chemistry, 2016, 27, 1707-1712.	3.6	73
39	Influence of 24-Nor-Ursodeoxycholic Acid on Hepatic Disposition of [18F]Ciprofloxacin, a Positron Emission Tomography Study in Mice. Journal of Pharmaceutical Sciences, 2016, 105, 106-112.	3.3	5
40	Generation and Characterization of a Breast Cancer Resistance Protein Humanized Mouse Model. Molecular Pharmacology, 2016, 89, 492-504.	2.3	23
41	[18F]FE@SUPPY: a suitable PET tracer for the adenosine A3 receptor? An in vivo study in rodents. European Journal of Nuclear Medicine and Molecular Imaging, 2015, 42, 741-749.	6.4	5
42	Factors Governing P-Glycoprotein-Mediated Drug–Drug Interactions at the Blood–Brain Barrier Measured with Positron Emission Tomography. Molecular Pharmaceutics, 2015, 12, 3214-3225.	4.6	39
43	[18F]FDG is not transported by P-glycoprotein and breast cancer resistance protein at the rodent blood–brain barrier. Nuclear Medicine and Biology, 2015, 42, 585-589.	0.6	2
44	Development of Fluorine-18 Labeled Metabolically Activated Tracers for Imaging of Drug Efflux Transporters with Positron Emission Tomography. Journal of Medicinal Chemistry, 2015, 58, 6058-6080.	6.4	18
45	Automated electrophilic radiosynthesis of [18F]FBPA using a modified nucleophilic GE TRACERlab FXFDG. Applied Radiation and Isotopes, 2015, 104, 124-127.	1.5	9
46	Development and performance test of an online blood sampling system for determination of the arterial input function in rats. EJNMMI Physics, 2015, 2, 1.	2.7	22
47	Automated radiosynthesis of [18F]ciprofloxacin. Applied Radiation and Isotopes, 2015, 99, 133-137.	1.5	5
48	Breast Cancer Resistance Protein and P-Glycoprotein Influence In Vivo Disposition of <sup>11</sup> C-Erlotinib. Journal of Nuclear Medicine, 2015, 56, 1930-1936.	5.0	52
49	Development of a <sup>18</sup> F‣abeled Tetrazine with Favorable Pharmacokinetics for Bioorthogonal PET Imaging. Angewandte Chemie - International Edition, 2014, 53, 9655-9659.	13.8	108
50	Radiosynthesis of [124I]Iodometomidate and Biological Evaluation Using Small-Animal PET. Molecular Imaging and Biology, 2014, 16, 317-321.	2.6	5
51	Preclinical in vitro & in vivo evaluation of [11C]SNAP-7941 – the first PET tracer for the melanin concentrating hormone receptor 1. Nuclear Medicine and Biology, 2013, 40, 919-925.	0.6	20
52	(R)-[11C]verapamil is selectively transported by murine and human P-glycoprotein at the blood–brain barrier, and not by MRP1 and BCRP. Nuclear Medicine and Biology, 2013, 40, 873-878.	0.6	67
53	Tariquidar and Elacridar Are Dose-Dependently Transported by P-Glycoprotein and Bcrp at the Blood-Brain Barrier: A Small-Animal Positron Emission Tomography and In Vitro Study. Drug Metabolism and Disposition, 2013, 41, 754-762.	3.3	79
54	Assessment of cerebral P-glycoprotein expression and function with PET by combined [11C]inhibitor and [11C]substrate scans in rats. Nuclear Medicine and Biology, 2013, 40, 755-763.	0.6	15

THOMAS WANEK

#	Article	IF	CITATIONS
55	Radioligands targeting Pâ€glycoprotein and other drug efflux proteins at the blood–brain barrier. Journal of Labelled Compounds and Radiopharmaceuticals, 2013, 56, 68-77.	1.0	45
56	A Novel PET Protocol for Visualization of Breast Cancer Resistance Protein Function at the Blood–Brain Barrier. Journal of Cerebral Blood Flow and Metabolism, 2012, 32, 2002-2011.	4.3	46
57	Interaction of HM30181 with P-glycoprotein at the murine blood–brain barrier assessed with positron emission tomography. European Journal of Pharmacology, 2012, 696, 18-27.	3.5	9
58	Synthesis and preclinical evaluation of the radiolabeled P-glycoprotein inhibitor [11C]MC113. Nuclear Medicine and Biology, 2012, 39, 1219-1225.	0.6	17
59	The antiepileptic drug mephobarbital is not transported by P-glycoprotein or multidrug resistance protein 1 at the blood–brain barrier: A positron emission tomography study. Epilepsy Research, 2012, 100, 93-103.	1.6	12
60	A comparative small-animal PET evaluation of [11C]tariquidar, [11C]elacridar and (R)-[11C]verapamil for detection of P-glycoprotein-expressing murine breast cancer. European Journal of Nuclear Medicine and Molecular Imaging, 2012, 39, 149-159.	6.4	23
61	Radiosynthesis and Assessment of Ocular Pharmacokinetics of 124I-Labeled Chitosan in Rabbits Using Small-Animal PET. Molecular Imaging and Biology, 2011, 13, 222-226.	2.6	19
62	Radiosynthesis and in vivo evaluation of 1-[18F]fluoroelacridar as a positron emission tomography tracer for P-glycoprotein and breast cancer resistance protein. Bioorganic and Medicinal Chemistry, 2011, 19, 2190-2198.	3.0	30
63	Gastric Cancer Growth Control by BEZ235 <i>In Vivo</i> Does Not Correlate with PI3K/mTOR Target Inhibition but with [18F]FLT Uptake. Clinical Cancer Research, 2011, 17, 5322-5332.	7.0	33
64	A Novel Positron Emission Tomography Imaging Protocol Identifies Seizure-Induced Regional Overactivity of P-Glycoprotein at the Blood-Brain Barrier. Journal of Neuroscience, 2011, 31, 8803-8811.	3.6	58
65	Dose-response assessment of tariquidar and elacridar and regional quantification of P-glycoprotein inhibition at the rat blood-brain barrier using (R)-[11C]verapamil PET. European Journal of Nuclear Medicine and Molecular Imaging, 2010, 37, 942-953.	6.4	102
66	Synthesis and in vivo evaluation of [11C]tariquidar, a positron emission tomography radiotracer based on a third-generation P-glycoprotein inhibitor. Bioorganic and Medicinal Chemistry, 2010, 18, 5489-5497.	3.0	73
67	Small-animal PET evaluation of [11C]MC113 as a PET tracer for P-glycoprotein. BMC Pharmacology, 2010, 10, .	0.4	0
68	Evaluation of [11C]elacridar and [11C]tariquidar in transporter knockout mice using small-animal PET. NeuroImage, 2010, 52, S25.	4.2	3
69	Synthesis and in vivo evaluation of the putative breast cancer resistance protein inhibitor [11C]methyl 4-((4-(2-(6,7-dimethoxy-1,2,3,4-tetrahydroisoquinolin-2-yl)ethyl)phenyl)amino-carbonyl)-2-(quinoline-2-carbonyla Nuclear Medicine and Biology, 2010, 37, 637-644.	mi <b>o</b> œ)benz	zoatæ.
70	Limitations of Small Animal PET Imaging with [18F]FDDNP and FDG for Quantitative Studies in a Transgenic Mouse Model of Alzheimer's Disease. Molecular Imaging and Biology, 2009, 11, 236-240.	2.6	87
71	Synthesis and Small-Animal Positron Emission Tomography Evaluation of [11C]-Elacridar As a Radiotracer to Assess the Distribution of P-Glycoprotein at the Bloodâ <sup>~'</sup> Brain Barrier. Journal of Medicinal Chemistry, 2009, 52, 6073-6082.	6.4	71
72	Synthesis of a [ <sup>18</sup> F]fluorobenzothiazole as potential amyloid imaging agent. Journal of Labelled Compounds and Radiopharmaceuticals, 2008, 51, 137-145.	1.0	14

#	Article	IF	CITATIONS
73	Tariquidar-Induced P-Glycoprotein Inhibition at the Rat Blood–Brain Barrier Studied with ( <i>R</i> )- <sup>11</sup> C-Verapamil and PET. Journal of Nuclear Medicine, 2008, 49, 1328-1335.	5.0	104
74	Pre vivo, ex vivo and in vivo evaluations of [68Ga]-EDTMP. Nuclear Medicine and Biology, 2007, 34, 391-397.	0.6	37